



Journal of Applied and Computational Mechanics



Research Paper

Numerical Simulations of Unsteady 3D MHD Micropolar Fluid Flow over a Slendering Sheet

S.R.R. Reddy¹, P.B. Anki Reddy²

¹ Department of Mathematics, SAS, Vellore Institute of Technology, Vellore-632014, India, Email: reddyshekara43@gmail.com

² Department of Mathematics, SAS, Vellore Institute of Technology, Al-Kharj, Saudi Arabia, Email: pbarmaths@gmail.com

Received September 12 2019; Revised November 11 2019; Accepted for publication January 09 2020.

Corresponding author: P.B. Anki Reddy (pbarmaths@gmail.com)

© 2018 Published by Shahid Chamran University of Ahvaz

Abstract. The purpose of the present analysis is to explore the numerical investigation on the time-dependent 3D magnetohydrodynamic flow of micropolar fluid over a slendering stretchable sheet. The prevailing PDEs are rehabilitated into coupled non-linear ODEs with the aid of appropriate similarity variables and then numerically calculated by applying the 4th RKM incorporate with shooting scheme. The contributions of various interesting variables are shown graphically. Emerging physical parameters on velocity, microrotation, and the surface drag coefficient are portrayed graphically. It is noticed that the microrotation profiles highly influenced by the vortex viscosity parameter and the micro-inertia density parameter. It is also concluded that the microrotation profiles (h_2) are promoted by increasing the spin gradient viscosity parameter. Excellent accuracy of the present results is observed with the formerly published as a result of a special case.

Keywords: MHD; Slendering stretchable sheet; Micropolar fluid; Time-dependent 3D flow; Numerical solution.

1. Introduction

Fluid flow over a stretching surface has been effectively contemplated for decades owing to its wide range applications such as extrude plastic sheets, cooling of metallic sheets or metal chips, artificial fibers, drawing of copper wires, MHD generators, paper manufacturing, liquid film-wise condensation processes, glass-forming technique, metal turning and many others. The concept of micropolar fluid and its uses to the motion of suspension solutions were conferred by Ahmadi [1]. The combined effects of viscoelasticity and a magnetic field over a stretching surface were prepared by Andersson [2]. The effect of Arrhenius activation on hydromagnetic Eyring-Powell nanofluid flow towards a stretched sheet was analyzed by Reddy et al. [3]. Acharya et al. [4] investigated the effect of hydromagnetic on Ag-water and TiO₂-water nanofluid over a varying movable surface. Reddy et al. [5] explored the impact of non-uniform heat source/sink and chemical reaction on the magneto-fluid dynamics blood flow over an inclined permeable stretching surface with an acute angle α to the vertical surface. The hydromagnetic three-dimensional free convective flow of nanofluid over an exponentially stretching sheet with chemical reaction was developed by Nayak et al. [6]. Sundry investigators [7-16] inspected the distinct flow problems over a stretching surface.

The interesting aspects of micropolar fluids can be found in the books of Eringen [17]. It has been presented a field of dynamic research because of their applications in numerous procedures that arise in the industry. Cases of these applications incorporate the flow of expulsion of polymer fluids, body fluids, intriguing ointments, materials processing, creature blood, polymeric fabrication, solidification of fluid precious stones, colloidal suspensions and numerous different circumstances. Eringen [18] improved his hypothesis of simple micro fluids to consider the thermal effects (heat conduction and heat dissipation). An analysis has been done to acquire the impacts of chemically reactive species in a permeable medium of micropolar fluid flow on a nonlinear porous extended sheet with variable concentration of the reactant that was developed by Rahman and Al-Lawatia [19]. Srinivas et al. [20] explored the combined effects of



thermal radiation and chemical reaction on the unsteady flow of a micropolar fluid over a stretching sheet embedded in a non-Darcian permeable medium. More recently, Gupta et al. [21] employed a finite element approach to examine the mixed convective flow of micropolar fluid over a permeable contracting sheet with an influence of Lorentz force. Many authors explored the importance of micropolar fluid with free, forced and mixed convection over various geometries. [22-32]. The micromotion of fluid components, spin inertia and the impacts of the couple stresses are significant in micropolar fluids.

Magnetic fields are inexhaustibly utilized as a part of different assembling procedures, for example, MHD control generators, pumps, and stream meters, in the design of the cooling framework, purification of molten metals from metallic incorporations with liquid metals, etc. The magneto-fluid dynamics flow and heat transfer over an extending sheet had been considered by Kumari et al. [33]. It is noticed that the wall temperature, Prandtl number, and the sink notably affects the heat exchanger. At the point $m < -2$ and $Pr > 2.5$ the implausible temperature distribution is encountered. Attia [34] examined the impact of Lorentz force on a time-dependent non-newtonian micropolar fluid over a permeable disk and observed that the Lorentz force highly dominates the fluid velocity and temperature. Recently Khan et al. [35] numerically explored the Williamson nanofluid behavior over a variable extending surface with an influence of an inclined magnetic field and assumed that the variable viscosity varies as a linear function of temperature.

The objective of this study is to numerical investigation on the unsteady three-dimensional MHD flow of micropolar over a slendering stretchable sheet. The current work determinations are to accomplish this gap in the existing literature. Such type of studies finds their vigorous applications in polymer fluids, body fluids, exotic lubricants, animal blood, solidification of liquid crystals, electronic chips, artificial fibres, drawing of copper wires, oceanography, artificial fibres, etc.

2. Mathematical Modeling

Let us consider the time-dependent 3D magnetohydrodynamic flow of a micropolar fluid over a slendering extensible surface. The surface is not flat and has been portrayed with a given profile indicated as $z = J(1 - mt)^{1/2}(x + y + c)^{(1-n)/2}$ here, $m \geq 0$. In this problem, the velocity power index $n \neq 1$ and J are assumed to be too small to satisfy the sheet with a pressure gradient along with the sheet. The coordinate scheme and flow model as exposed in Fig. 1.

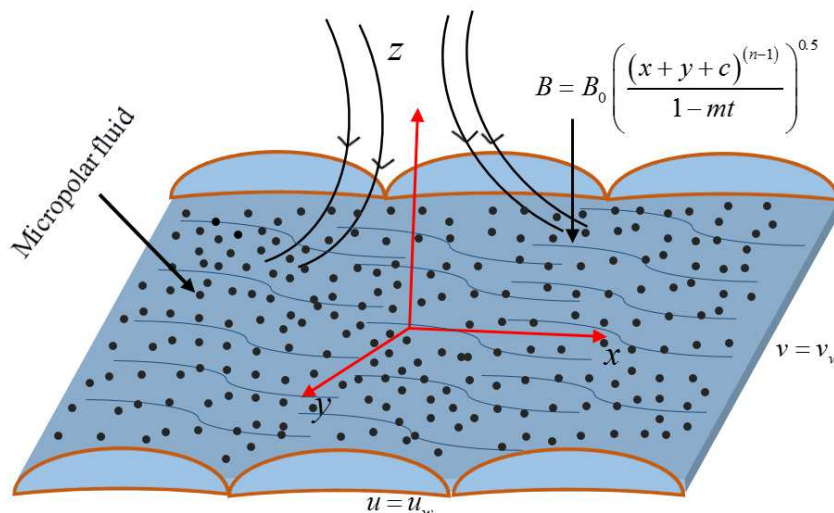


Fig. 1 Physical configuration of the problem.

At the time $t = 0$, the sheet is impulsively stretched. The magnetic field B is applied vertically to the sheet. Under these assumptions, the governing equations are specified in the vectorial form as (see Ahmad et al. [30])

$$\rho \frac{\partial \mathbf{V}}{\partial t} + \nabla \cdot (\rho \mathbf{V}) = 0, \quad (1)$$

$$\rho \frac{d\mathbf{V}}{dt} = (\lambda + 2\mu + \kappa) \nabla (\nabla \cdot \mathbf{V}) - (\mu + \kappa) \nabla \times (\nabla \times \mathbf{V}) - \kappa \nabla \times \boldsymbol{\omega} - \nabla p + \mathbf{J} \times \mathbf{B}, \quad (2)$$

$$\rho j \frac{d\boldsymbol{\omega}}{dt} = \kappa \nabla \times \mathbf{V} - 2\kappa \boldsymbol{\omega} + (\alpha + \beta + \gamma) \nabla (\nabla \cdot \boldsymbol{\omega}) - \gamma \nabla \times \nabla \times \boldsymbol{\omega} \quad (3)$$

where κ is the vortex viscosity, \mathbf{V} is the velocity vector, ρ is the fluid density, $\boldsymbol{\omega}$ is the microrotation vector, λ , α and β



are the new viscosity coefficients for micropolar fluids, $J \equiv \sigma(V \times B)$ is the current density in which B is the magnetic field strength, $j = 2\nu / u_w$ is the micro-inertia per unit mass, μ is the viscosity of the classical viscous fluid, σ denotes the electrical conductivity of the fluid. The fluid begins to move abruptly from the plain sheet at $t = 0$ when the flat sheet expands in two horizontal ways. Using the standard boundary-layer approximations, based on the scale investigation, the governing equations yield the following (See Chamkha et al. [29] and Subhani and Nadeem [31])

$$\frac{\partial u}{\partial x} + \frac{\partial v}{\partial y} + \frac{\partial w}{\partial z} = 0, \quad (4)$$

$$\frac{\partial u}{\partial t} + u \frac{\partial u}{\partial x} + v \frac{\partial u}{\partial y} + w \frac{\partial u}{\partial z} = \left(\frac{\mu + \kappa}{\rho} \right) \frac{\partial^2 u}{\partial z^2} - \frac{\kappa}{\rho} \left(\frac{\partial \omega_2}{\partial z} \right) - \frac{\sigma B^2}{\rho} u, \quad (5)$$

$$\frac{\partial v}{\partial t} + u \frac{\partial v}{\partial x} + v \frac{\partial v}{\partial y} + w \frac{\partial v}{\partial z} = \left(\frac{\mu + \kappa}{\rho} \right) \frac{\partial^2 v}{\partial z^2} + \frac{\kappa}{\rho} \left(\frac{\partial \omega_1}{\partial z} \right) - \frac{\sigma B^2}{\rho} v, \quad (6)$$

$$\left(\frac{\partial \omega_1}{\partial t} + u \frac{\partial \omega_1}{\partial x} + v \frac{\partial \omega_1}{\partial y} + w \frac{\partial \omega_1}{\partial z} \right) \rho j = \chi \frac{\partial^2 \omega_1}{\partial z^2} - \kappa \left(2\omega_1 + \frac{\partial v}{\partial z} \right), \quad (7)$$

$$\left(\frac{\partial \omega_2}{\partial t} + u \frac{\partial \omega_2}{\partial x} + v \frac{\partial \omega_2}{\partial y} + w \frac{\partial \omega_2}{\partial z} \right) \rho j = \chi \frac{\partial^2 \omega_2}{\partial z^2} - \kappa \left(2\omega_2 - \frac{\partial u}{\partial z} \right), \quad (8)$$

The boundary conditions are

$$\left. \begin{aligned} u = u_w, \quad v = v_w, \quad w = 0, \quad \omega_1 = l \frac{\partial v}{\partial z}, \quad \omega_2 = -l \frac{\partial u}{\partial z} \quad \text{at } z = J(1 - mt)^{0.5}(x + y + c)^{\frac{(1-n)}{2}} \\ u \rightarrow 0, \quad v \rightarrow 0, \quad \omega_1 \rightarrow 0, \quad \omega_2 \rightarrow 0 \quad \text{as } z \rightarrow \infty \end{aligned} \right\} \quad (9)$$

where

$$u_w = U_0 \frac{(x + y + c)^n}{1 - mt}, \quad B = B_0 \left(\frac{(x + y + c)^{(n-1)}}{1 - mt} \right)^{\frac{1}{2}}, \quad v_w = U_0 \frac{(x + y + c)^n}{1 - mt}, \quad (10)$$

Here, the spin gradient viscosity χ is assumed to be constant and given by

$$\chi = \left(\frac{\kappa}{2} + \mu \right) j \quad (11)$$

We now introduced the following similarity transformations (see Acharya et al. [4])

$$\left. \begin{aligned} \zeta &= \left(\frac{(n+1)U_0}{2\nu(1-mt)} \right)^{\frac{1}{2}} (x + y + c)^{\frac{(n-1)}{2}} z, \quad u = U_0 \frac{(x + y + c)^n}{1 - mt} F'(\zeta), \quad v = U_0 \frac{(x + y + c)^n}{1 - mt} G'(\zeta), \\ \omega_1 &= \left(\frac{U_0}{1 - mt} \right)^{\frac{3}{2}} \left(\frac{(n+1)}{2\nu} \right)^{\frac{1}{2}} (x + y + c)^{\frac{(3n-1)}{2}} H_1(\zeta), \quad \omega_2 = \left(\frac{U_0}{1 - mt} \right)^{\frac{3}{2}} \left(\frac{(n+1)}{2\nu} \right)^{\frac{1}{2}} (x + y + c)^{\frac{(3n-1)}{2}} H_2(\zeta), \\ w &= - \left(\frac{2\nu U_0}{(n+1)(1-mt)} \right)^{\frac{1}{2}} (x + y + c)^{\frac{(n-1)}{2}} \left[\zeta (F'(\zeta) + G'(\zeta)) \frac{n-1}{2} + (F(\zeta) + G(\zeta)) \frac{n+1}{2} \right], \end{aligned} \right\} \quad (12)$$

Substituting (12) into Eqs. (5)-(8), we get the following equations:

$$F'''(1 + R_1) - \left(\frac{A}{n+1} \right) (\zeta F'' + 2F') - \frac{2n}{n+1} F'(F' + G') + F''(F + G) - R_1 H_2' - \frac{2M}{n+1} F' = 0, \quad (13)$$

$$G'''(1 + R_1) - \left(\frac{A}{n+1} \right) (\zeta G'' + 2G') - \frac{2n}{n+1} G'(F' + G') + G''(F + G) + R_1 H_1' - \frac{2M}{n+1} G' = 0, \quad (14)$$



$$R_2 H_1'' - \left(\frac{A}{n+1} \right) (\zeta H_1' + 3H_1) - \left(\frac{3n-1}{n+1} \right) H_1 (F' + G') + H_1' (F + G) - \left(\frac{2R_1 R_3}{n+1} \right) (2H_1 + G'') = 0, \quad (15)$$

$$R_2 H_2'' - \left(\frac{A}{n+1} \right) (\zeta H_2' + 3H_2) - \left(\frac{3n-1}{n+1} \right) H_2 (F' + G') + H_2' (F + G) - \left(\frac{2R_1 R_3}{n+1} \right) (2H_2 - F'') = 0, \quad (16)$$

where A, R_1, R_2, R_3 and M are the unsteadiness parameter, vortex viscosity parameter, spin gradient viscosity parameter, micro-inertia density parameter, and magnetic parameter respectively, which are given by

$$M = \frac{\sigma B_0^2}{\rho U_0}, R_1 = \frac{\kappa}{\mu}, R_2 = \frac{\chi}{\mu j}, R_3 = \frac{\nu}{u_w j(x+y+c)}, A = \frac{m}{U_0} (x+y+c)^{1-n}, \quad (17)$$

In this paper, R_3 and A are treated as the local dimensionless parameters, which have a fixed incentive in the specific condition of the sheet.

The corresponding boundary conditions are

$$\left. \begin{aligned} F(\zeta) &= \lambda \left(\frac{1-n}{1+n} \right), G(\zeta) = \lambda \left(\frac{1-n}{1+n} \right), F'(\zeta) = 1, \\ G'(\zeta) &= 1, H_1(\zeta) = l G''(\zeta), H_2(\zeta) = -l F''(\zeta), \\ F'(\zeta) &= 0, G'(\zeta) = 0, H_1(\zeta) = 0, H_2(\zeta) = 0. \end{aligned} \right\} \begin{aligned} &at \ \zeta = \lambda \\ &as \ \zeta \rightarrow \infty \end{aligned} \quad (18a)$$

where ' denotes the differentiation with respect to ζ and $\lambda = J((n+1)U_0 / 2\nu)^{1/2}$ is a variable of the wall thickness. Let us define

$$\begin{aligned} F(\zeta) &= f(\zeta - \lambda) = f(\eta), \\ G(\zeta) &= g(\zeta - \lambda) = g(\eta), \\ H_1(\zeta) &= h_1(\zeta - \lambda) = h_1(\eta), \\ H_2(\zeta) &= h_2(\zeta - \lambda) = h_2(\eta). \end{aligned} \quad (18b)$$

Substituting the above expressions into Eqs. (13)-(18), which become as,

$$f'''(1+R_1) - \left(\frac{A}{n+1} \right) ((\eta + \lambda) f'' + 2f') - \frac{2n}{n+1} f'(f' + g') + f''(f + g) - R_1 h_2' - \frac{2M}{n+1} f' = 0, \quad (19)$$

$$g'''(1+R_1) - \left(\frac{A}{n+1} \right) ((\eta + \lambda) g'' + 2g') - \frac{2n}{n+1} g'(f' + g') + g''(f + g) + R_1 h_1' - \frac{2M}{n+1} g' = 0, \quad (20)$$

$$R_2 h_1'' - \left(\frac{A}{n+1} \right) ((\eta + \lambda) h_1' + 3h_1) - \left(\frac{3n-1}{n+1} \right) h_1 (f' + g') + h_1' (f + g) - \left(\frac{2R_1 R_3}{n+1} \right) (2h_1 + g'') = 0, \quad (21)$$

$$R_2 h_2'' - \left(\frac{A}{n+1} \right) ((\eta + \lambda) h_2' + 3h_2) - \left(\frac{3n-1}{n+1} \right) h_2 (f' + g') + h_2' (f + g) - \left(\frac{2R_1 R_3}{n+1} \right) (2h_2 - f'') = 0, \quad (22)$$

with the boundary conditions,

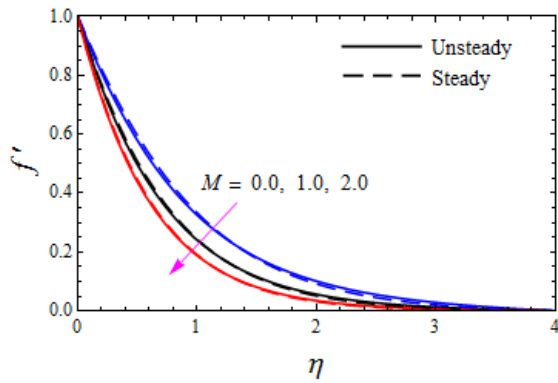
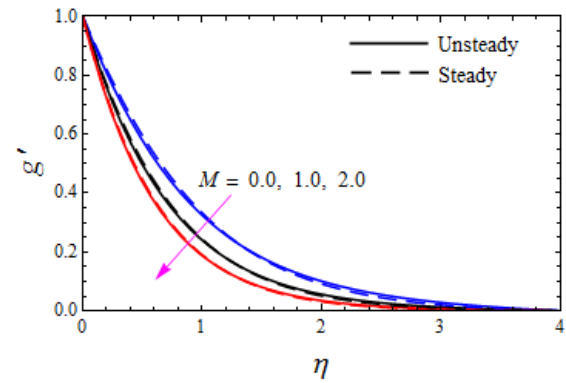
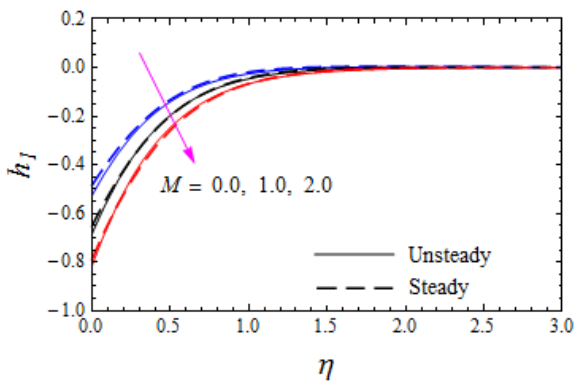
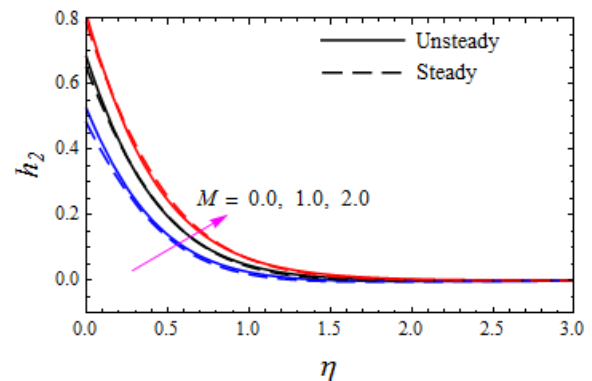
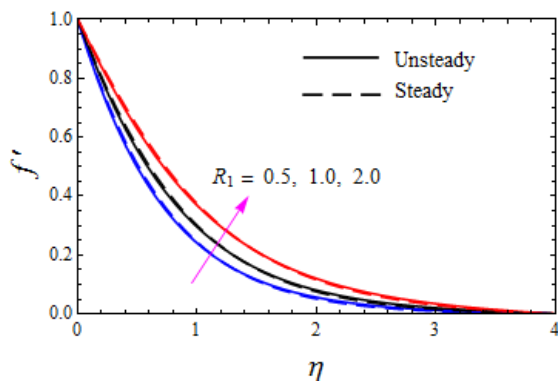
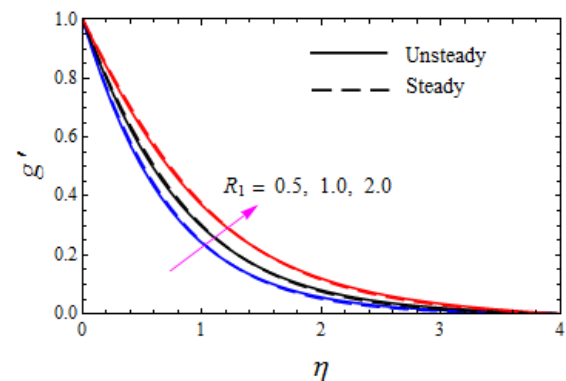
$$\left. \begin{aligned} f(0) &= \lambda \left(\frac{1-n}{1+n} \right), g(0) = \lambda \left(\frac{1-n}{1+n} \right), f'(0) = 1, \\ g'(0) &= 1, h_1(0) = l g''(0), h_2(0) = -l f''(0), \\ f'(\infty) &= 0, g'(\infty) = 0, h_1(\infty) = 0, h_2(\infty) = 0. \end{aligned} \right\} \quad (23)$$

Among physical quantities of interest, skin friction coefficients are

$$\left. \begin{aligned} C_{f_{xz}} \text{Re}_x^{1/2} &= 2 \left(\frac{1+n}{2} \right)^{0.5} [1 + (1-l)R_1] f''(0), \\ C_{f_{yz}} \text{Re}_x^{1/2} &= 2 \left(\frac{1+n}{2} \right)^{0.5} [1 + (1+l)R_1] g''(0). \end{aligned} \right\} \quad (24)$$

where $\text{Re}_x = u_w(x+y+c)/\nu$ is the local Reynolds number.

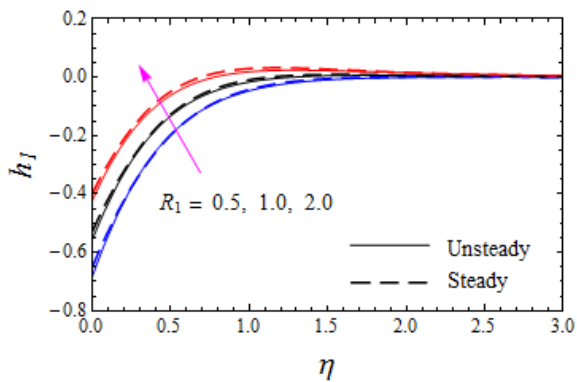
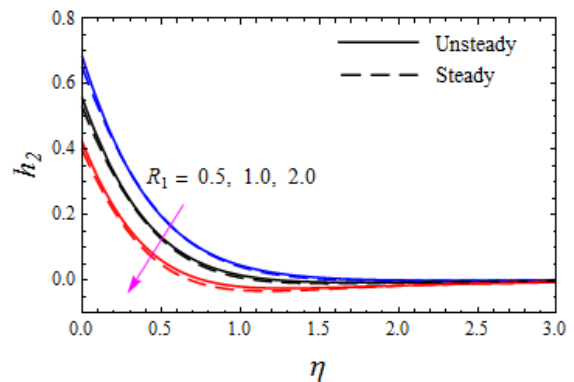
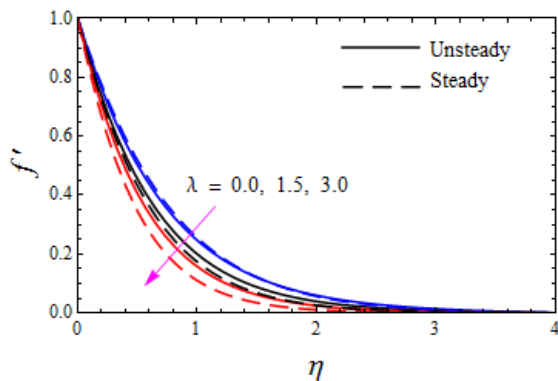
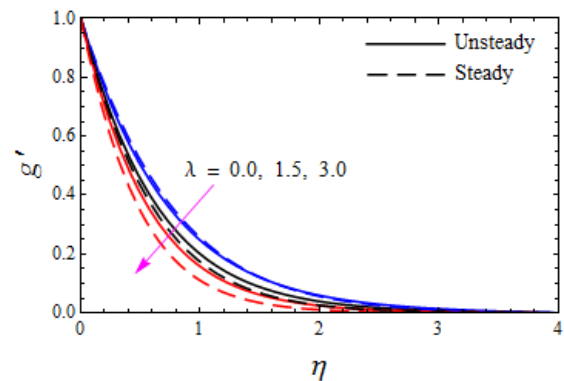
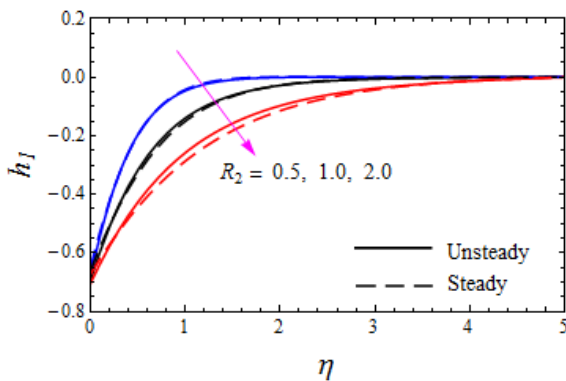
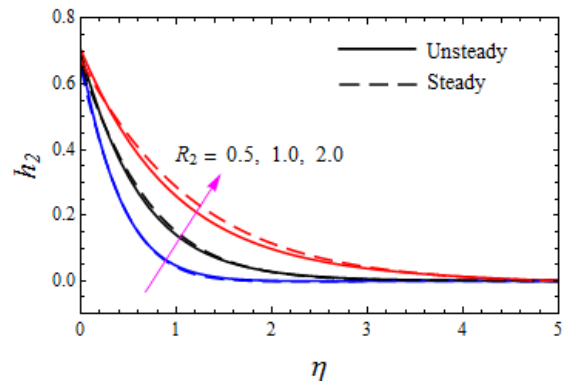


Fig. 2. Increasing values of M on f' .Fig. 3. Increasing values of M on g' .Fig. 4. Increasing values of M on h_1 .Fig. 5. Increasing values of M on h_2 .Fig. 6. Increasing values of R_1 on f' .Fig. 7. Increasing values of R_1 on g' .

3. Results and Discussions

The influence of numerous parameters is reconnoitered on the fluid velocities, microrotation profiles for both $A = 0$ and $A = 0.5$ cases, which are portrayed in Figs. 2-19. If $A = 0$ then the mathematical represents steady case and $A = 0.5$ then the mathematical represents the unsteady case. It is shown through Figs. 2-5 the impact of magnetic parameter M on velocity and microrotation distributions in the x - and y -directions. When the magnetic parameter increases, the velocity magnitudes ($f(\eta)$ and $g(\eta)$) of the fluid for x - and y -directions become lower as seen through Figs. 2 and 3. An increment in the magnetic parameter from $M = 0$ to $M > 0$ effects to decrease the velocity because of presence in an electrically conducting fluid familiarize with impeding body force acting toward the direction of the applied magnetic field. Since the presence of the magnetic parameter interrupts the flow of the fluid, the velocity of the fluid decreases. Fig. 4 exhibits that the reduced microrotation profiles h_1 in the y -direction are negative and decreases in absolute value with M but the boundary layer thickness diminishes with the increase of M . Finally, we noticed that the reduced microrotation profiles h_2 increase with M as can be seen from Fig. 5. The boundary layer thickness reduces as the great moves away from the wall. In electroconductive polymer processing, the intensity of rotatory motions of the suspensions (microelements) is therefore also successfully controlled with the imposition of a magnetic field. This is particularly important in applications where homogenous distributions of microelements are needed.



Fig. 8. Increasing values of R_1 on h_1 .Fig. 9. Increasing values of R_1 on h_2 .Fig. 10. Increasing values of λ on f' .Fig. 11. Increasing values of λ on g' .Fig. 12. Increasing values of R_2 on h_1 .Fig. 13. Increasing values of R_2 on h_2 .

Figures 6-9 demonstrate the variations on $f'(\eta)$, $g'(\eta)$, $h_1(\eta)$ and $h_2(\eta)$ microrotation with a dissimilarity of $R_1 = \kappa / \mu$, the material parameter it gives the ratio between dynamic viscosity and vortex viscosity of the fluid under consideration. These two viscosities have a similar in R_1 . It was found out about the speed that it overhauls with an extension in R_1 as appeared in Figs. 6-7. This is a result of the vortex thickness that impacts liquid particles to quicken while the magnetic field slows down the flow. It is evident from this accept the thickness of the boundary layer ascends with R_1 . As we increase R_1 the absolute value of the velocity gradient close to the surface drops. Fig. 8 demonstrates that the reduced microrotation profiles h_1 in the y -direction is negative and decreases in absolute value with R_1 but the boundary layer thickness decreases with the increase of R_1 . Finally, we noticed that the reduced microrotation profiles h_2 increment with R_1 as can be seen from Fig. 9. Figs. 10-11 demonstrate the variations on $f'(\eta)$ and $g'(\eta)$ microrotation with a dissimilarity of λ . From these figures, it is revealed that the velocities decrease with rising in λ for the cases of $A = 0$ and $A = 0.5$.



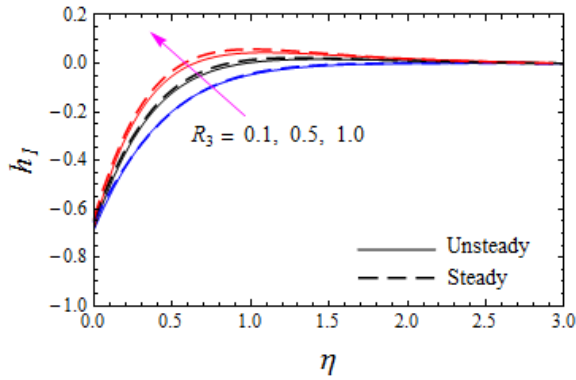


Fig. 14. Increasing values of R_3 on h_1 .

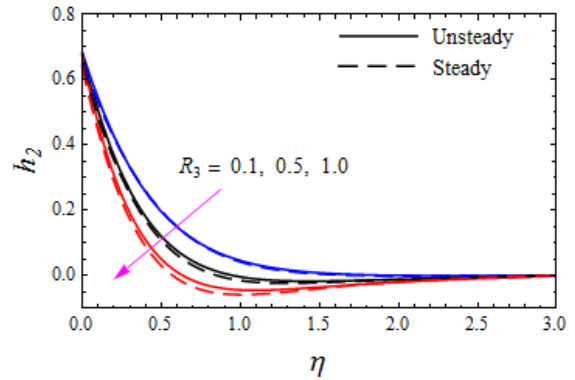


Fig. 15. Increasing values of R_3 on h_2 .

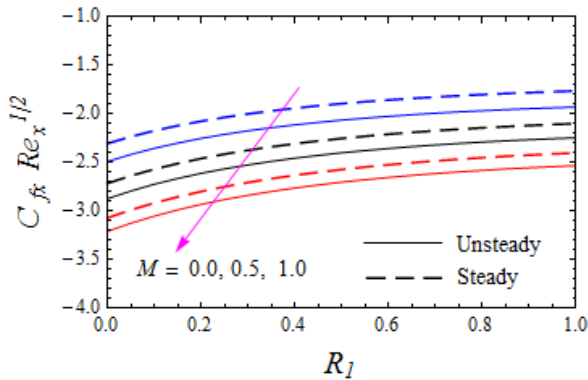


Fig. 16. Increasing values of M on $C_{fx} Re_x^{1/2}$.

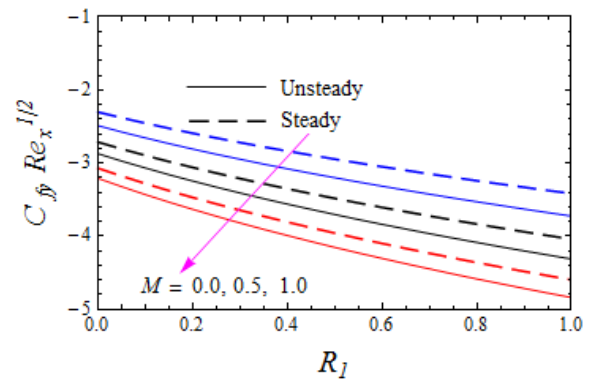


Fig. 17. Increasing values of M on $C_{fy} Re_x^{1/2}$.

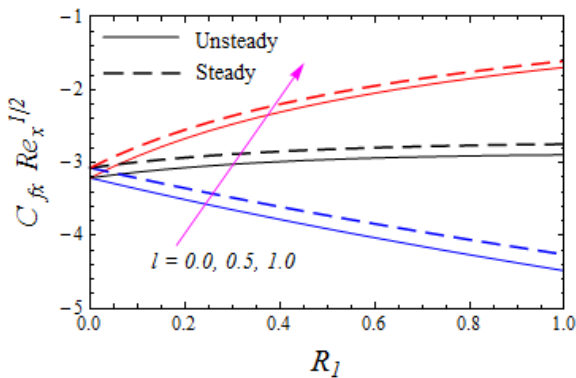


Fig. 18. Increasing values of l on $C_{fx} Re_x^{1/2}$.

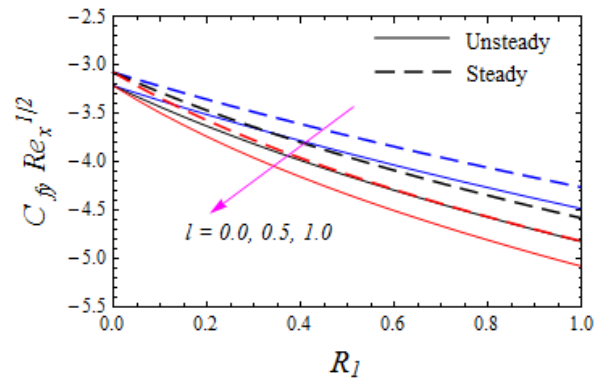


Fig. 19. Increasing values of l on $C_{fy} Re_x^{1/2}$.

Table 1. Comparison $-f''(0)$ for various values of n with $A = 0$, $M = 0$, $R_I = 0$, $R_2 = 0$, $R_3 = 0$, $l = 0$.

n	Fang et al. [15]	Khader and Megahed [12]	Present results
10	1.0603	1.0603	1.06034
5	1.0486	1.0486	1.04862
3	1.0359	1.0358	1.03588
2	1.0234	1.0234	1.02342
1	1.0000	1.0000	1.00000
0.5	0.9799	0.9798	0.97994
0	0.9576	0.9577	0.95764
-0.5	1.1667	1.1666	1.16666

The impact of the spin gradient viscosity parameter on the velocity profiles is delineated in Figs. 12-13. From Fig. 12, the velocity profile is reduced with a growing spin gradient viscosity parameter for the $A = 0$ and $A = 0.5$ cases. An increasing the values of the spin gradient viscosity parameter, boosts the velocity profile for the $A = 0$ and $A = 0.5$ cases. Figs. 14-15 delineate the velocity profiles for numerous estimations of the micro-inertia density parameter. From Fig. 14,



we found that a growing the velocity profile by increasing micro-inertia density for $A = 0$ and $A = 0.5$ cases. Figure 15 displays the impact of the micro-inertia density parameter on the velocity profile. It is seen from this figure that the fluid velocity drops with increasing values of the micro-inertia density parameter for the $A = 0$ and $A = 0.5$ cases, respectively. The impact of the magnetic parameter (M) on the $C_{fx} \text{Re}_x^{1/2}$ and $C_{fy} \text{Re}_x^{1/2}$ is portrayed in Figs. 16-17. From these Figs, the $C_{fx} \text{Re}_x^{1/2}$ and $C_{fy} \text{Re}_x^{1/2}$ are found to reduce with the rise in the magnetic parameter for both $A = 0$ and $A = 0.5$ cases. Figs. 18-19 exemplify the $C_{fx} \text{Re}_x^{1/2}$ and $C_{fy} \text{Re}_x^{1/2}$ for various estimations of the boundary. Here we saw from Fig. 18 that builds the $C_{fx} \text{Re}_x^{1/2}$, by expanding the boundary parameter for both $A = 0$ and $A = 0.5$ cases. From Fig. 19, we found that the $C_{fy} \text{Re}_x^{1/2}$ drops with expanding the estimations of the boundary parameter for both $A = 0$ and $A = 0.5$ cases.

4. Conclusion

A numerical solution was exhibited for the unsteady, three-dimensional hydromagnetic flow of a micropolar fluid over a slendering stretchable sheet with thermal radiation. 4th RKM incorporate with shooting scheme was employed to solve this present model. The main interpretations from this investigation can be abridged as follows

- The velocity profiles diminish with the higher value of the magnetic parameter for the cases of steady and unsteady.
- Flow equations are highly nonlinear and coupled in the domain $[\lambda, \infty)$.
- The skin friction coefficient decreases with the rise in the magnetic parameter.
- The velocity profiles strengthen by means of the vortex viscosity parameter for both the cases.

Author Contributions

S.R.R. Reddy developed the mathematical modeling, examined the numerical validation and analyzed the empirical results. P. Bala Anki Reddy initiated the project and developed the numerical scheme for solving the mathematical model. Both the authors have discussed the results, reviewed and approved the final version of the manuscript.

Conflict of Interest

The authors declared no potential conflicts of interest with respect to the research, authorship and publication of this article.

Funding

The authors received no financial support for the research, authorship and publication of this article.

Nomenclature

A	Unsteadiness parameter	σ	The electrical conductivity of the fluid
M	Magnetic parameter	κ	Vortex viscosity
R_1	Vortex viscosity parameter	j	Micro-inertia per unit mass
Re	Reynolds number	ρ	The density of the fluid
u, v, w	The components of velocities in x, y and z directions	χ	Spin gradient viscosity
R_3	The micro-inertia density parameter	ω	Microrotation vector
J	Current density	ω_1, ω_2	The components of the microrotation vectors to the ω
B	Magnetic field strength	λ, α, β	The spin viscosity coefficients for micropolar fluid
R_2	The spin gradient viscosity parameter	ζ	Similarity variable
n	Velocity power index parameter	ψ	Stream function

Greek Symbols

μ Dynamic viscosity

References

- [1] Ahmadi, G., Self-similar solution of incompressible micropolar boundary layer flow over a semi-infinite plate, *Int. J. Eng. Sci.*, 14, 1976, 639–646.
- [2] Andersson, H.I., MHD flow of a viscoelastic fluid past a stretching surface, *Acta Mech.*, 95, 1992, 227–230.
- [3] Reddy, S.R.R., Bala Anki Reddy, P., Bhattacharyya, K., Effect of nonlinear thermal radiation on 3D magneto slip flow of Eyring-Powell nanofluid flow over a slendering sheet with binary chemical reaction and Arrhenius activation



energy, *Adv. Powder Technol.*, 2019, 1-11, in press.

- [4] Acharya, N., Das, K., Kumar Kundu, P., Ramification of variable thickness on MHD TiO₂ and Ag nanofluid flow over a slendering stretching sheet using NDM, *Eur. Phys. J. Plus.*, 131, 2016, 1–16.
- [5] Reddy, S.R.R., Bala Anki Reddy, P., Suneetha, S., Magnetohydrodynamic flow of blood in a permeable inclined stretching surface with viscous dissipation, non-uniform heat source/sink and chemical reaction, *Front. Heat Mass Transf.*, 10, 2018, 1–10.
- [6] Nayak, M.K., Akbar, N.S., Tripathi, D., Khan, Z.H., Pandey, V.S., MHD 3D free convective flow of nanofluid over an exponentially stretching sheet with chemical reaction, *Adv. Powder Technol.*, 28, 2017, 2159–2166.
- [7] Srinivas, S., Reddy, P.B.A., Prasad, B.S.R. V., Effects of Chemical Reaction and Thermal Radiation on Mhd Flow Over an Inclined Permeable Stretching Surface With Non-Uniform Heat Source/Sink: an Application To the Dynamics of Blood Flow, *J. Mech. Med. Biol.*, 14, 2014, 1–24.
- [8] Rashad, A.M., Impact of thermal radiation on MHD slip flow of a ferrofluid over a non-isothermal wedge, *J. Magn. Magn. Mater.*, 422, 2017, 25–31.
- [9] Reddy, P.B.A., Suneetha, S., Effects of homogeneous-heterogeneous chemical reaction and slip velocity on MHD stagnation flow of a micropolar fluid over a permeable stretching/shrinking surface embedded in a porous medium, *Front. Heat Mass Transf.*, 8, 2017, 1–11.
- [10] Reddy, P.B.A., MHD boundary layer slip flow of a Casson fluid over an exponentially stretching surface in the presence of thermal radiation and chemical reaction, *J. Nav. Archit. Mar. Eng.*, 3, 2016, 165–177.
- [11] Pal, D., Roy, N., Vajravelu, K., Effects of thermal radiation and Ohmic dissipation on MHD Casson nanofluid flow over a vertical non-linear stretching surface using scaling group transformation, *Int. J. Mech. Sci.*, 114, 2016, 257–267.
- [12] Khader, M.M., Megahed, A.M., Numerical solution for boundary layer flow due to a nonlinearly stretching sheet with variable thickness and slip velocity, *Eur. Phys. J. Plus.*, 128, 2013, 1–7.
- [13] Soomro, F.A., Haq, R. ul, Khan, Z.H., Zhang, Q., Passive control of nanoparticle due to convective heat transfer of Prandtl fluid model at the stretching surface, *Chinese J. Phys.*, 55, 2017, 1561–1568.
- [14] Hosseini, E., Loghmani, G.B., Heydari, M., Rashidi, M.M., Numerical investigation of velocity slip and temperature jump effects on unsteady flow over a stretching permeable surface, *Eur. Phys. J. Plus.*, 132, 2017, 1–16.
- [15] Fang, T., Zhang, J., Zhong, Y., Boundary layer flow over a stretching sheet with variable thickness, *Appl. Math. Comput.*, 218, 2012, 7241–7252.
- [16] Bala Anki Reddy, P., Magnetohydrodynamic flow of a Casson fluid over an exponentially inclined permeable stretching surface with thermal radiation and chemical reaction, *Ain Shams Eng. J.*, 7, 2016, 593–602.
- [17] Eringen, A.C., Theory of Micropolar Fluids, *J. Math. Mech.*, 16, 1966, 1–18.
- [18] Eringen, A.C., Theory of thermomicrofluids, *J. Math. Anal. Appl.*, 38, 480–496.1972,
- [19] Rahman, M.M., Al-Lawatia, M., Effects of higher-order chemical reaction on micropolar fluid flow on a power-law permeable stretched sheet with variable concentration in a porous medium, *Can. J. Chem. Eng.*, 88, 2010, 23–32.
- [20] Srinivas, S., Reddy, P.B.A., Prasad, B.S.R.V., Non-Darcian unsteady flow of a micropolar fluid over a porous stretching sheet with thermal radiation and chemical reaction, *Heat Transf. Res.*, 44, 2015, 172–187.
- [21] Gupta, D., Kumar, L., Anwar Bé, O., Singh, B., Finite Element Analysis of MHD Flow of Micropolar Fluid over a Shrinking Sheet with a Convective Surface Boundary Condition, *J. Eng. Thermophys.*, 27, 2018, 202–220.
- [22] Ayano, M.S., Sikwila, S.T., Shateyi, S., MHD Mixed Convection Micropolar Fluid Flow through a Rectangular Duct, *Math. Probl. Eng.*, 2018, 2018, 1–8.
- [23] Ibrahim, S.M., Kumar, V., Raju, C.S.K., Possessions of viscous dissipation on radiative MHD heat and mass transfer flow of a micropolar fluid over a porous stretching sheet with chemical reaction, *Transp. Phenom. Nano Macro Scales.*, 6, 2018, 60–71.
- [24] Shamshuddin, M.D., Satya Narayana, P.V., Primary and secondary flows on unsteady MHD free convective micropolar fluid flow past an inclined plate in a rotating system: A finite element analysis, *Fluid Dyn. Mater. Process.*, 14, 2018, 57–86.
- [25] Pal, D., Mandal, G., Thermal radiation and MHD effects on boundary layer flow of micropolar nanofluid past a stretching sheet with non-uniform heat source/sink, *Int. J. Mech. Sci.*, 126, 2017, 308–318.
- [26] Reddy, P.B.A., Sekhar, D.V., Effects of radiation on MHD mixed convection flow of a micropolar fluid over a heated stretching surface with heat generation/absorption, *Int. J. Eng. Res. Appl.*, 3, 2013, 572–581.
- [27] Gnaneswara Reddy, M., Reddy, G.R.S., Micropolar fluid flow over a nonlinear stretching convectively heated vertical surface in the presence of Cattaneo-Christov heat flux and viscous dissipation, *Front. Heat Mass Transf.*, 8, 2017, 1–9.
- [28] Ramzan, M., Chung, J.D., Ullah, N., Partial slip effect in the flow of MHD micropolar nanofluid flow due to a rotating disk – A numerical approach, *Results Phys.*, 7, 2017, 3557–3566.
- [29] Chamkha, A.J., Jaradat, M., Pop, I., Three-Dimensional Micropolar Flow due to a Stretching Flat Surface, *Int. J. Fluid Mech. Res.*, 30, 2003, 357–366.
- [30] Ahmad, K., Nazar, R., Ishak, A., Pop, I., Unsteady three-dimensional boundary layer flow due to a stretching surface in amicropolar fluid, *Int. J. Numer. Methods Fluids*, 68, 2012, 1561–1573.
- [31] Subhani, M., Nadeem, S., Numerical analysis of 3D micropolar nanofluid flow induced by an exponentially stretching surface embedded in a porous medium, *Eur. Phys. J. Plus.*, 132, 2017, 1–12.
- [32] Mabood, F., Ibrahim, S.M., Rashidi, M.M., Shadloo, M.S., Lorenzini, G., Non-uniform heat source/sink and Soret




effects on MHD non-Darcian convective flow past a stretching sheet in a micropolar fluid with radiation, *Int. J. Heat Mass Transf.*, 93, 2016, 674–682.


[33] Kumari, M., Takhar, H.S., Nath, G., MHD flow and heat transfer over a stretching surface with prescribed wall temperature or heat flux, *Heat & Mass Transfer*, 25, 1990, 331–336.

[34] Attia, H.A., Unsteady MHD flow near a rotating porous disk with uniform suction or injection, *Fluid Dyn. Res.*, 23, 1998, 283–290.

[35] Khan, M., Malik, M.Y., Salahuddin, T., Hussian, A., Heat and mass transfer of Williamson nanofluid flow yield by an inclined Lorentz force over a nonlinear stretching sheet, *Results Phys.*, 8, 2018, 862–868.

ORCID iD

S.R.R. Reddy  <https://orcid.org/0000-0001-5501-570X>

P. Bala Anki Reddy  <https://orcid.org/0000-0001-5824-1796>



© 2020 Shahid Chamran University of Ahvaz, Ahvaz, Iran. This article is an open access article distributed under the terms and conditions of the Creative Commons Attribution-NonCommercial 4.0 International (CC BY-NC 4.0 license) (<http://creativecommons.org/licenses/by-nc/4.0/>).

How to cite this article: Reddy S.R.R., Anki Reddy P.B. Numerical Simulations of Unsteady 3D MHD Micropolar Fluid Flow over a Slendering Sheet, *J. Appl. Comput. Mech.*, 7(3), 2021, 1403–1412.
<https://doi.org/10.22055/JACM.2020.31062.1821>

Publisher's Note Shahid Chamran University of Ahvaz remains neutral with regard to jurisdictional claims in published maps and institutional affiliations.

